CRYSTAL GROWTH & DESIGN

COMMUNICATION

pubs.acs.org/crystal

Growth of Rutile Titanium Dioxide Nanowires by Pulsed Chemical Vapor Deposition

Jian Shi and Xudong Wang*

Department of Materials Science and Engineering, University of Wisconsin—Madison, 1509 University Avenue, Madison, Wisconsin 53706, United States

ABSTRACT: Recently, we developed a surface reaction-limited pulsed chemical vapor deposition (CVD) technique that can grow highly uniform anatase TiO_2 nanorods (NRs) over a large area, even inside highly confined submicrometer-sized spaces. Here, we report the growth of rutile TiO_2 NWs using this technique by introducing a Au seeding layer at higher deposition temperature, where a small amount of anatase phase was also found. A bifurcated growth of rutile TiO_2 NWs was observed. The resulting TiO_2 NWs exhibited high-quality crystallinity and large surface areas with exposure of high-index surfaces. Control experiments illustrated the influence of deposition conditions on the TiO_2 growth behavior. Higher deposition temperature could convert the TiO_2 phase from anatase to rutile. A thin film of Au was able to induce rapid crystal growth resulting in particle formation, while the anisotropic NW growth preferred no Au coating. Shorter purging time could significantly enhance the deposition rate because of the incomplete removal of precursor molecules. This research enriched our knowledge of the surface reaction-limited pulsed CVD technique and demonstrated the capability of using this technique to control the TiO_2 phase and morphology.

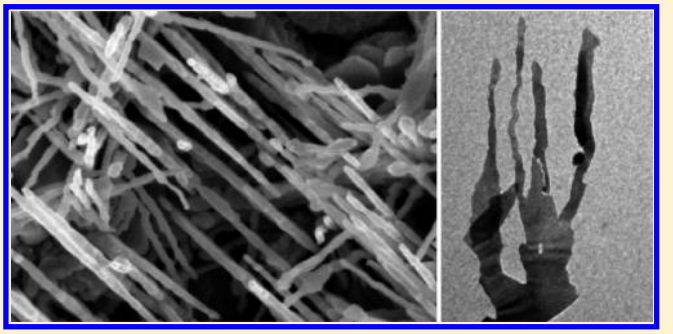

Titanium dioxide (TiO_2), due to its excellent solid-state physical−chemical properties, has demonstrated a wide range of applications in hydrogen production, lithium-ion batteries, fuel cells, gas sensors, detoxification, photovoltaics, photocatalysts, and supercapacitors.[1−13] The one-dimensional (1D) morphology, such as a TiO_2 nanowire (NW), is considered as a superior candidate for achieving higher performance in those applications compared to the bulk form.[4,6,8,11−13] For example, a TiO_2 NW-based electrode can provide a large surface area for effectively collecting photons and/or electrons.[4] The high crystal quality of the NWs is essential to reduce the scattering effect and hence improve the electron mobility compared to the porous TiO_2 films composed of nanosized particles. In addition, using TiO_2 NWs as electrodes could be beneficial to the mechanical stability of the device.[2,4] Typically, TiO_2 exhibits three different polymorphs (anatase, brookite, and rutile), which have different properties and result in different performance. Therefore, to synthesize TiO_2 nanostructures with defined phase, shape, dimension, and high quality crystallinity is of fundamental importance for achieving desired functionality and performance.

Nonetheless, a well-controlled growth of TiO_2 NW is rather challenging due to the existence of multiple polymorphs and the thermodynamically unfavorable crystallography for anisotropic crystal growth, particularly with large aspect ratio.[14,15] The templated sol−gel method, hydrothermal synthesis, and electrospinning process have been demonstrated for creating the NW morphology.[16−19] However, phase-purity/selectivity, crystallinity, and impurity involvement are typical concerns of these methods.[20] Post-heat-treatment is always needed to improve the crystallinity of NWs. On the other hand, high-temperature deposition can achieve high crystal quality. TiO_2 NWs have also been grown by a chemical vapor deposition (CVD) process.[21,22] However, large-scale, controlled synthesis of TiO_2 NWs via vapor deposition is still a challenge due to the extremely low vapor pressure (10^{-3} Torr at 1577 °C) and high melting point of Ti, that result in a very small and sensitive deposition condition window for the formation of the TiO_2 NW morphology.[21] Recently, our group demonstrated a surface reaction-limited pulsed CVD technique that can grow highly uniform anatase TiO_2 nanorods (NRs) over a large area, even inside highly confined submicrometer-sized spaces.[23] This technique has the potential to achieve a large-scale synthesis of TiO_2 1D nanostructure arrays with controlled dimensions and phases. In this paper, we report the growth of rutile TiO_2 NWs through this technique in a clean and controllable manner. A bifurcated growth of TiO_2 NWs was observed. The resulting TiO_2 NWs exhibited curvy and high-index surfaces. Control experiments further illustrated the effect of purging time, Au coating, and temperature on the product phase and morphology. This research enriched our knowledge on the recently developed surface

Received: January 27, 2011
Revised: February 22, 2011
Published: March 01, 2011

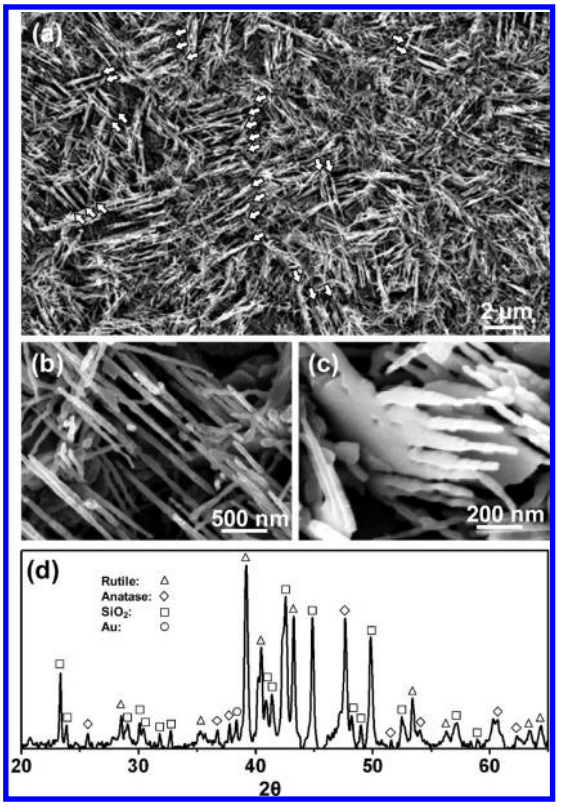

Figure 1. (a) Overview SEM image of TiO_2 nanostructures grown on Au coated Si substrate. The quasi-aligned nanostructure arrays are indicated by white arrows. (b) Top view of the array of the NWs-on-flake structure showing a parallel arrangement. (c) A tilted image showing the NWs-on-flake structure. (d) X-ray diffraction spectrum of the as-synthesized TiO_2 nanostructures.

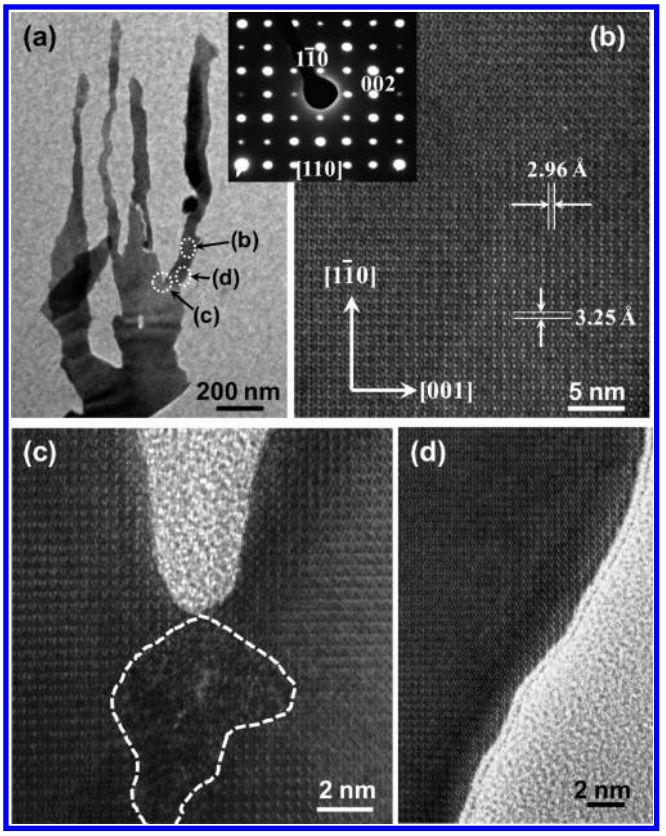

Figure 2. TEM analysis of the NWs-on-flake structure. (a) A single piece of the NWs-on-flake structure. The inset is the SAED pattern confirming the single-crystalline rutie phase. (b−d) HRTEM images acquired from the NW body, the bifurcation region, and the curvy edge of the NWs-on-flake structure, respectively, as highlighted by white dashed circles in part a.

reaction-limited CVD technique and demonstrated the capability of using this technique to control the TiO_2 phase and morphology.

The rutile TiO_2 NWs were synthesized in a homemade atomic layer deposition (ALD) system at 650 °C using $TiCl_4$ and H_2O as the precursors. In a typical experiment, a (100) oriented silicon wafer was cleaned with acetone, ethanol, and DI water and dried with nitrogen gas. A thin layer of Au (∼5 nm) was sputtered on the Si surface to facilitate the NW nucleation. This substrate was loaded into the ALD chamber, where a constant flow of 40 sccm N_2 was applied as the carrier gas. The precursors were preheated to a temperature of 80 °C before entering the growth chamber. The pulsing times for $TiCl_4$ and H_2O were both 4 s; and the purging times were 10 s. The typical growth cycles ranged from a few hundred to a few thousand. After the growth, the chamber was cooled to room temperature naturally and the samples were removed for investigation.

Figure 1a is a low magnification scanning electron microscopy (SEM) image showing the as-grown TiO_2 NWs on silicon substrate. The entire substrate was covered by a large quantity of NWs, where short-range alignments of the NWs can be observed. As indicated by white arrows in Figure 1a, the aligned NW region typically consisted of a few rugged strips that were parallel to each other. Both the distance between neighboring strips and the width of each strip were around a few hundred nanometers. This local alignment phenomenon indicates that the parallel strips were likely originated from a crystallized film underneath. The morphology of strips with NWs is shown in Figure 1b. The strips were composed of a group of NWs with approximately the same orientation. The NWs were a few micrometers long and exhibit a fairly uniform thickness of ∼30 nm. In addition, large pieces of film underneath could also be observed. The tilted image of the NW sample revealed that the aligned arrays were actually packed TiO_2 flakes with spaced NWs grown on the top side, where several NWs with rough surfaces and nonuniform widths could be clearly seen growing along the same orientation. These NWs shared the same thickness as the base flakes, while their widths decreased from the bottom (∼100 nm) to the tip (∼20−30 nm). The lengths of those NWs were typically 1−2 μm. Observation across the entire substrate revealed that most NWs belonged to this morphology.

The as-synthesized TiO_2 nanostructures were found to have both rutile and anatase phases, as confirmed by X-ray diffraction (XRD) (Figure 1d). Most noticeable peaks in this XRD spectrum were indexed to rutile TiO_2 (ICSD No. 062679) phase, anatase TiO_2 (ICSD No. 063711), and SiO_2 (ICSD No. 081381) phase. The appearance of SiO_2 phase was possibly due to the reaction between the H_2O vapor and Si substrate at high temperature (650 °C) during the growth. The Au (111) peak was observed as well.

Transmission electron microscopy (TEM) images shown in Figure 2a clearly revealed the NWs-on-flake structure and the curvy side surfaces of these NWs. This configuration suggests that the NWs were most likely formed by bifurcations of the flake matrix. Each bifurcation produced two branches as the newly formed small flakes or NWs. The branching took place at

dx.doi.org/10.1021/cg200140k |*Cryst. Growth Des.* 2011, 11, 949–954

different vertical positions along the flakes until the width of the new flake became smaller than 100 nm, and thus, the NW morphology was received. The single-crystalline structure was confirmed by the selective-area electron diffraction (SAED) pattern shown in the inset of Figure 2a. The flat flake surface was the (110) facet, and the NWs were grown along the [1$\bar{1}$0] direction. The high-resolution TEM (HRTEM) image reveals the perfect crystal structure of the NWs, as shown in Figure 2b. The uniform lattice pattern and contrast indicate the NWs had a very uniform thickness. The lattice spacing measured from Figure 2b and the lattice constants calculated from the SAED pattern further confirmed the rutile phase of the NWs. This high-quality lattice structure was found consistent over the entire flake-NW structure except the bifurcation regions. As shown in Figure 2c, poor crystallinity was observed at the region where two NWs sprout apart (circled by the white dashed lines). The two NWs still maintained perfect single crystal integrity with the flake. This poor crystalline region was typically around 20−30 nm and exhibited an irregular shape. No anatase phase was observed from the TiO_2 NW/flake structure collected from the as-synthesized samples. Noting that discontinuous Au coverage is typical for a thin film of Au catalyst at high temperature,[24] we believe the anatase phase was most likely formed on the substrate where the surface is not covered by Au, which is similar to the results in our previous study. The anatase phase could thus be easily buried under the large amount of rutile nanostructures.

Different from most other single crystal NW morphologies made by either hydrothermal or vapor deposition approaches, which usually consisted of low-index flat surfaces, the as-received rutile TiO_2 NWs showed curvy side surfaces,[17,21] whereas no dislocations were observed, as shown in Figure 2d. The uniform contrast also indicates the thickness along the curved edge was still uniform. Such curved side surfaces consist of high-index crystal facets and thus render much higher surface energy compared to the low-index facets, which, as a result, might enhance the catalytic activity of the TiO_2 NWs.

It should to be noted that our synthesis used separated $TiCl_4$ and H_2O precursors. Previous analyses have shown that the anisotropic growth relies on a long purging time (60 s) in order to effectively remove the remaining precursor molecules. A shorter purging time would leave a significant amount of residual precursor vapor and facilitate the isotropic CVD growth.[23,25] In these experiments, a shorter purging time (10 s) and higher deposition temperature (650 °C) were applied compared to our previous processes. Thus, the quantity and dimension of the deposited TiO_2 nanostructures were both significantly larger than those deposited with longer purging time (>60 s). This observation evidenced an enhanced CVD process due to the reduction of purging time.

Further experiments were conducted to reveal the effect of Au on the growth of TiO_2 nanostructures. Using Si substrates without Au coating, the pulsed CVD growth was performed at longer purging time (60 s) and with other deposition conditions unchanged. Short NRs were received covering the entire Si substrate surface after 1000 growth cycles (Figure 3a). The NRs were typically a few hundred nanometers long and tens of nanometers wide. Most of them had a rectangular cross section (inset of Figure 3a). This morphology was consistent with our previously reported growth observation of anatase TiO_2 NRs. Due to the higher deposition temperature (650 °C) and long growth period, the rutile phase was identified by XRD as the dominating phase (Figure 3b). Meanwhile, anatase and SiO_2

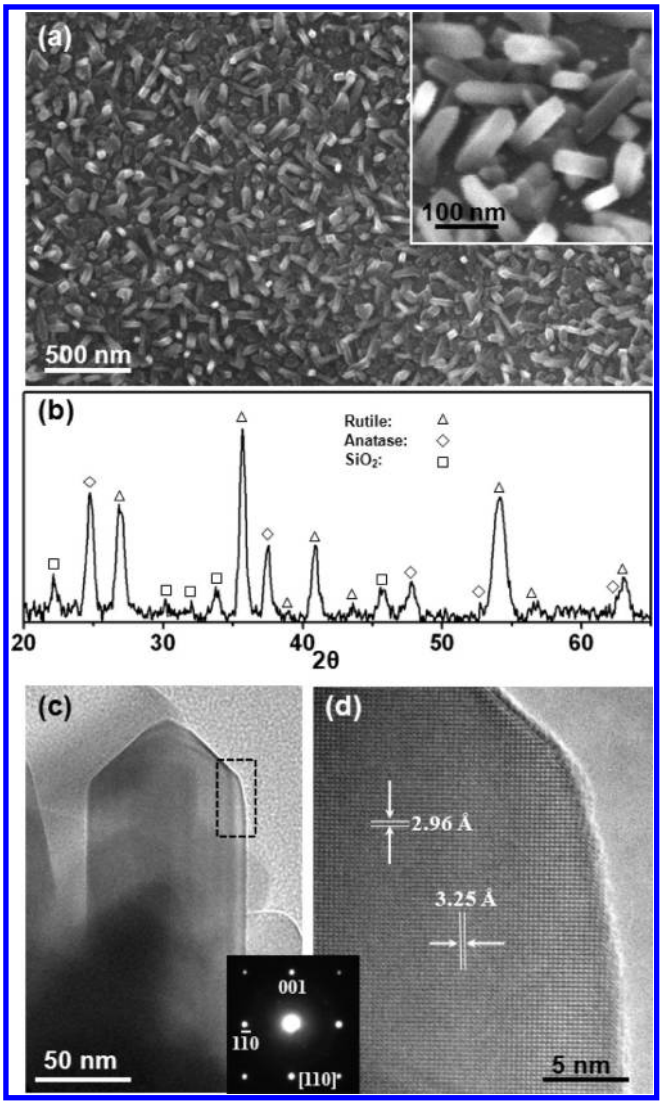

Figure 3. (a) Overview image of TiO_2 NRs grown on bare Si substrate with a purging time of 60 s. The inset is the magnified image of the TiO_2 NRs. (b) XRD spectrum of the TiO_2 NRs sample shown in part a. (c) TEM image of a TiO_2 NR. The inset is the corresponding SAED pattern confirming the rutile phase. (d) HRTEM image of a nanorod acquired from the rectangle region in part c.

phases were also observed. This phase information is consistent with the bifurcated NW structure. The TEM image showed that the TiO_2 NRs had a typically swordlike shape (Figure 3c).[15] The single-crystalline rutile structure was confirmed by the SAED pattern as shown in the inset of Figure 3c. Sharp surfaces and the dislocation-free lattice of rutile TiO_2 NRs can be identified by the HRTEM image shown in Figure 3d. The SEM images, SAED pattern, and HRTEM image together revealed that the NR was grown along the [001] direction and surrounded by four equivalent {110} surfaces. This experiment showed that simply increasing the deposition temperature and prolonging the growth period could change the phase of TiO_2 NRs from anatase to rutile but had negligible influence on the NR morphology. Therefore, it is likely that the formation of the bifurcated TiO_2 NWs was related to the presence of Au.

In order to further test this hypothesis, we performed two series of controlled experiments. First, a pulsed CVD growth of

dx.doi.org/10.1021/cg200140k |*Cryst. Growth Des.* 2011, 11, 949–954

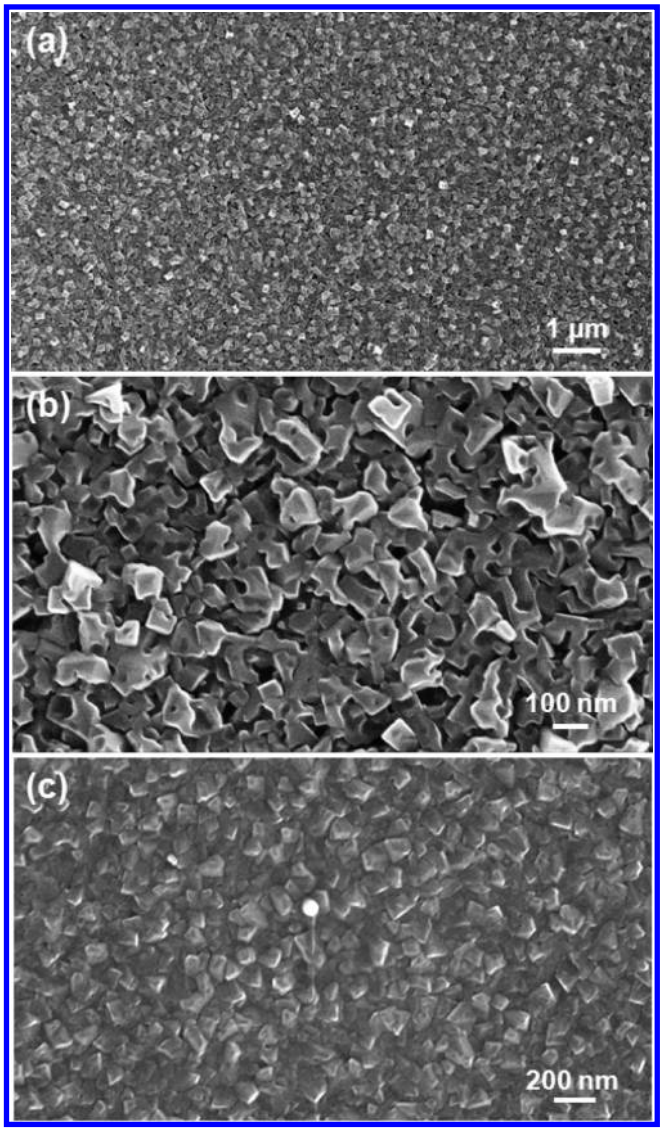

Figure 4. (a) SEM images of the TiO_2 crystal film grown on Au coated Si substrate with a purging time of 60 s. (b) Closer observation of the TiO_2 film features. (c) TiO_2 nanoparticles grown on bare Si substrate with a purging time of 10 s.

TiO_2 was conducted on a Au coated Si substrate using longer purging time but keeping other deposition conditions the same as that of rutile TiO_2 NR growth. After 1000 cycle deposition, no NR morphology could be observed by SEM. Instead, a quasi-continuous TiO_2 film was received (Figure 4a). Closer observation showed that the TiO_2 films were formed by crystals that merged together, resulting in a rough surface and many open spaces in between. The 4-fold symmetry feature could still be observed at certain regions (Figure 4b). This result was consistent with the proposed pulsed CVD mechanism, where elongated purging time can significantly reduce the amount of precursor and thus limit the growth of nanostructures. Second, a pulsed CVD growth of TiO_2 was performed using short purging time (10 s) on bare Si substrate at 650 °C. Only TiO_2 nanoparticles were observed (Figure 4c), which is consistent with the experimental results from our previous study conducted at 600 °C.

From the control experiments, it is feasible to conclude that a thin layer of Au could facilitate the growth of crystalline TiO_2 films during a pulsed CVD process. If the precursor was sufficient during the deposition, the films could evolve into bifurcated NWs. If the precursor supply was limited, the filmlike morphology would not change. However, currently, it is still unclear about the exact role of Au during the growth. No Au was observed from the NWs by TEM after growth, suggesting that the Au was not likely acting as the catalyst for a vapor−liquid−solid growth. It might be possible that Au wetted Si at high temperature and created a large number of favorable sites on the surface for absorbing incoming molecules, thus facilitating 2D lateral growth. Nevertheless, this hypothesis needs further in-depth evaluation and is beyond the scope of this paper.

Table 1. Summary of the Growth Condition Related TiO_2 Nanomorphologies

temp	purging time	Au coating	phase	morphology
600 °C	>60 s	no	anatase	small NRs
650 °C	>60 s	no	rutile/anatase	small NRs
650 °C	>60 s	yes	rutile/anatase	crystal films
650 °C	10 s	yes	rutile/anatase	NWs on flakes
650 °C	10 s	no	rutile/anatase	nanoparticles

The deposition condition related to TiO_2 nanostructure growth is summarized in Table 1 to clearly illustrate their relationships. Comparing the first two conditions clearly shows that higher deposition temperature is the main reason for the formation of rutile phase, since it is thermodynamically more stable than anatase phase at higher temperature. Based on these observations, the formation of bifurcated rutile TiO_2 NWs is proposed as shown in Figure 5. At the initial growth stage, due to the existence of Au, TiO_2 crystal films were deposited on the surface of Si substrate. The exposed facets of the crystals were {110} and {001} (step (i) in Figure 5). When the Au was completely buried or consumed by the quick deposition of TiO_2 (owing to the short purging time), the crystal growth front was hindered, and the growth mode switched from 3D crystal growth to vertical 2D film growth. This would lead to the first time growth split, and rectangle TiO_2 stripes were epitaxially formed on the surface of TiO_2 crystals (setp (ii) in Figure 5). Further growth of the stripes would form vertical TiO_2 flakes. Due to their epitaxial relationship with the bottom crystal, these 2D flakes were parallel to each other. Since the bottom crystals had limited surface size and random orientation, the parallel flakes appeared as small arrays, where each array had the same orientation but the distribution of array orientation was random (Figure 1a). It should be noted that the growth front of the TiO_2 flakes was still able to bifurcate due to the limited ability to absorb precursor molecules following the mechanism of surface reaction-limited growth. Eventually, the flake bifurcated and shrank into a few 1D NWs (step (iii) in Figure 5). The bifurcation should occur randomly (or most likely one after the other) during the growth. Thus, the splitting points of the flake should appear at different positions along the length direction. This is consistent with our TEM observation (Figure 2a).

In summary, the surface reaction-limited CVD growth of TiO_2 nanostructures was investigated at higher temperature with the presence of Au. Higher deposition temperature converted the TiO_2 phase from anatase to rutile. A thin film of Au was found to be able to induce rapid crystal growth, resulting in particle formation, while the anisotropic NW growth preferred no Au coating. Shorter purging time could significantly enhance the deposition rate because of the incomplete removal of precursor molecules. The formation of a 1D TiO_2 nanostructure under

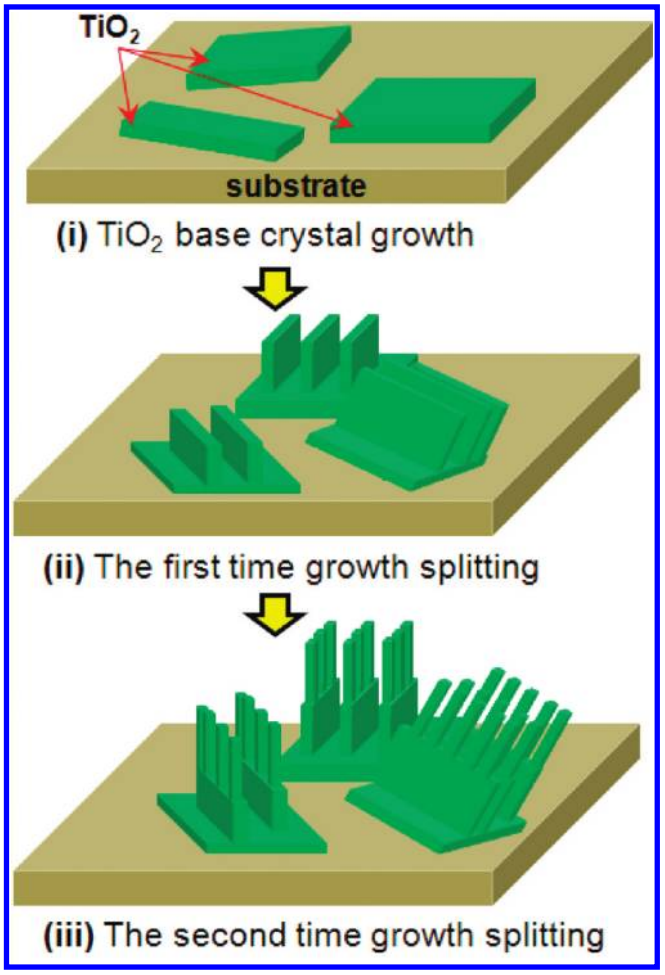

Figure 5. Proposed growth mechanism of the NWs-on-flake structure. (i) Growth of a TiO_2 crystal base film on a Si substrate assisted by Au film. (ii) Presence of the first set of bifurcation and the subsequent flake growth. (iii) Presence of the second set of bifurcation and the subsequent NWs growth.

shorter purging time was believed to be induced by the growth bifurcation, which might be a result of the surface reaction-limited CVD process. The bifurcated TiO_2 nanostructures showed high-quality crystallinity and large surface areas with exposure of high-index surfaces. This structure may render enhanced catalytic properties that would benefit from the applications of photovoltaic, photocatalysis, and energy storage systems. Understanding of the influence of temperature, Au deposition, and purging time on the growth behavior could largely enrich the knowledge of our recently developed surface reaction-limited pulsed CVD technique, leading toward a powerful scalable bottom-up nanostructure growth technique.

AUTHOR INFORMATION

Corresponding Author

*Phone: 608-890-2667. Fax: 608-262-8353. E-mail: xudong@engr.wisc.edu.

ACKNOWLEDGMENT

We thank the National Science Foundation under Grant No. CMMI-0926245 and University of Wisconsin—Madison graduate school.

REFERENCES

(1) Yang, H. G.; Sun, C. H.; Qiao, S. Z.; Zou, J.; Liu, G.; Smith, S. C.; Cheng, H. M.; Lu, G. Q. Anatase TiO2 single crystals with a large percentage of reactive facets. *Nature* **2008**, *453* (7195), 638–641.

(2) Jiu, J. T.; Isoda, S.; Wang, F. M.; Adachi, M. Dye-sensitized solar cells based on a single-crystalline TiO2 nanorod film. *J. Phys. Chem. B* **2006**, *110* (5), 2087–2092.

(3) Khan, S. U. M.; Al-Shahry, M.; Ingler, W. B. Efficient photochemical water splitting by a chemically modified n-TiO2 2. *Science* **2002**, *297* (5590), 2243–2245.

(4) Liu, B.; Aydil, E. S. Growth of Oriented Single-Crystalline Rutile TiO2 Nanorods on Transparent Conducting Substrates for Dye-Sensitized Solar Cells. *J. Am. Chem. Soc.* **2009**, *131* (11), 3985–3990.

(5) Hwang, Y. J.; Boukai, A.; Yang, P. D. High Density n-Si/n-TiO2 Core/Shell Nanowire Arrays with Enhanced Photoactivity. *Nano Lett.* **2009**, *9* (1), 410–415.

(6) Adachi, M.; Murata, Y.; Takao, J.; Jiu, J. T.; Sakamoto, M.; Wang, F. M. Highly efficient dye-sensitized solar cells with a titania thin-film electrode composed of a network structure of single-crystal-like TiO2 nanowires made by the "oriented attachment" mechanism. *J. Am. Chem. Soc.* **2004**, *126* (45), 14943–14949.

(7) Zuruzi, A. S.; Kolmakov, A.; MacDonald, N. C.; Moskovits, M. Highly sensitive gas sensor based on integrated titania nanosponge arrays. *Appl. Phys. Lett.* **2006**, *88* (10), 102904.

(8) Armstrong, A. R.; Armstrong, G.; Canales, J.; Garcia, R.; Bruce, P. G. Lithium-ion intercalation into TiO2-B nanowires. *Adv. Mater.* **2005**, *17* (7), 862–865.

(9) Liu, J. W.; Kuo, Y. T.; Klabunde, K. J.; Rochford, C.; Wu, J.; Li, J. Novel Dye-Sensitized Solar Cell Architecture Using TiO2-Coated Vertically Aligned Carbon Nanofiber Arrays. *ACS Appl. Mater. Interfaces* **2009**, *1* (8), 1645–1649.

(10) Ni, M.; Leung, M. K. H.; Leung, D. Y. C.; Sumathy, K. A review and recent developments in photocatalytic water-splitting using TiO2 for hydrogen production. *Renewable Sustainable Energy Rev.* **2007**, *11* (3), 401–425.

(11) Bach, U.; Lupo, D.; Comte, P.; Moser, J. E.; Weissortel, F.; Salbeck, J.; Spreitzer, H.; Gratzel, M. Solid-state dye-sensitized mesoporous TiO2 solar cells with high photon-to-electron conversion efficiencies. *Nature* **1998**, *395* (6702), 583–585.

(12) Law, M.; Greene, L. E.; Radenovic, A.; Kuykendall, T.; Liphardt, J.; Yang, P. D. ZnO-Al2O3 and ZnO-TiO2 core-shell nanowire dye-sensitized solar cells. *J. Phys. Chem. B* **2006**, *110* (45), 22652–22663.

(13) Greene, L. E.; Law, M.; Yuhas, B. D.; Yang, P. D. ZnO-TiO2 core-shell nanorod/P3HT solar cells. *J. Phys. Chem. C* **2007**, *111* (50), 18451–18456.

(14) Barnard, A. S.; Zapol, P. Predicting the energetics, phase stability, and morphology evolution of faceted and spherical anatase nanocrystals. *J. Phys. Chem. B* **2004**, *108* (48), 18435–18440.

(15) Barnard, A. S.; Curtiss, L. A. Prediction of TiO2 nanoparticle phase and shape transitions controlled by surface chemistry. *Nano Lett.* **2005**, *5* (7), 1261–1266.

(16) Miao, Z.; Xu, D. S.; Ouyang, J. H.; Guo, G. L.; Zhao, X. S.; Tang, Y. Q. Electrochemically induced sol-gel preparation of single-crystalline TiO2 nanowires. *Nano Lett.* **2002**, *2* (7), 717–720.

(17) Zhang, Y. X.; Li, G. H.; Jin, Y. X.; Zhang, Y.; Zhang, J.; Zhang, L. D. Hydrothermal synthesis and photoluminescence of TiO2 nanowires. *Chem. Phys. Lett.* **2002**, *365* (3−4), 300–304.

(18) Formo, E.; Lee, E.; Campbell, D.; Xia, Y. N. Functionalization of electrospun TiO2 nanofibers with Pt nanoparticles and nanowires for catalytic applications. *Nano Lett.* **2008**, *8* (2), 668–672.

(19) Hosono, E.; Fujihara, S.; Kakiuchi, K.; Imai, H. Growth of submicrometer-scale rectangular parallelepiped rutile TiO2 films in aqueous TiCl3 solutions under hydrothermal conditions. *J. Am. Chem. Soc.* **2004**, *126* (25), 7790–7791.

(20) Bavykin, D. V.; Friedrich, J. M.; Walsh, F. C. Protonated titanates and TiO2 nanostructured materials: Synthesis, properties, and applications. *Adv. Mater.* **2006**, *18* (21), 2807–2824.

(21) Wu, J. M.; Shih, H. C.; Wu, W. T.; Tseng, Y. K.; Chen, I. C. Thermal evaporation growth and the luminescence property of TiO2 nanowires. *J. Cryst. Growth* **2005**, *281* (2−4), 384–390.

(22) Amin, S. S.; Nicholls, A. W.; Xu, T. T. A facile approach to synthesize single-crystalline rutile TiO2 one-dimensional nanostructures. *Nanotechnology* **2007**, *18* (44), 445609–445609.

(23) Shi, J.; Sun, C.; Starr, M. B.; Wang, X. D. Growth of Titanium Dioxide Nanorods in 3D-Confined Spaces. *Nano Lett.* **2011**, *11* (2), 624−631.

(24) Wang, X. D.; Song, J. H.; Summers, C. J.; Ryou, J. H.; Li, P.; Dupuis, R. D.; Wang, Z. L. Density-controlled growth of aligned ZnO nanowires sharing a common contact: A simple, low-cost, and mask-free technique for large-scale applications. *J. Phys. Chem. B* **2006**, *110* (15), 7720–7724.

(25) Chen, C. A.; Chen, Y. M.; Korotcov, A.; Huang, Y. S.; Tsai, D. S.; Tiong, K. K. Growth and characterization of well-aligned densely-packed rutile TiO2 nanocrystals on sapphire substrates via metal-organic chemical vapor deposition. *Nanotechnology* **2008**, *19* (7), 075611–075611.